



The Selective Oxidation of Cyclohexane via In-situ H₂O₂ Production Over Supported Pd-based Catalysts

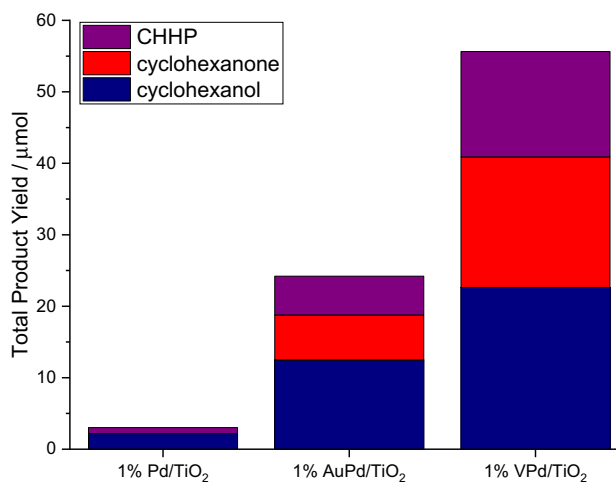
Caitlin M. Crombie¹ · Richard J. Lewis¹ · Dávid Kovačič¹ · David J. Morgan^{1,2} · Thomas J. A. Slater³ · Thomas E. Davies¹ · Jennifer. K. Edwards¹ · Martin Skov Skjøth-Rasmussen⁴ · Graham J. Hutchings¹

Received: 18 November 2020 / Accepted: 21 December 2020
© The Author(s) 2021

Abstract

The oxidation of cyclohexane via the in-situ production of H₂O₂ from molecular H₂ and O₂ offers an attractive route to the current industrial means of producing cyclohexanone and cyclohexanol (KA oil), key materials in the production of Nylon. The in-situ route has the potential to overcome the significant economic and environmental concerns associated with the use of commercial H₂O₂, while also allowing for the use of far lower reaction temperatures than those typical of the purely aerobic route to KA oil. Herein we demonstrate the efficacy of a series of bi-functional Pd-based catalysts, which offer appreciable concentrations of KA oil, under conditions where limited activity is observed using O₂ alone. In particular the introduction of V into a supported Pd catalyst is seen to improve KA oil concentration by an order of magnitude, compared to the Pd-only analogue. In particular we ascribe this improvement in catalytic performance to the development of Pd domains of mixed oxidation state upon V incorporation as evidenced through X-ray photoelectron spectroscopy.

Graphic Abstract



Keywords Palladium · Vanadium · Hydrogen peroxide · Cyclohexane oxidation · Green chemistry

Caitlin M. Crombie and Richard J. Lewis have contributed equally to this work.

Supplementary Information The online version contains supplementary material available at <https://doi.org/10.1007/s10562-020-03511-6>.

Extended author information available on the last page of the article

1 Introduction

The selective oxidation of cyclohexane is a key industrial route in the production of cyclohexanol and cyclohexanone (collectively termed KA oil), which are key feedstocks for adipic acid and caprolactam and ultimately Nylon-6,6 and

Nylon-6. Conventionally the industrial route to KA, via the high temperature (140–180 °C) aerobic oxidation of cyclohexane utilises homogeneous transition metal catalysts including cobalt [1, 2], chromium [3], or manganese [4], with conversion limited to around 5% to inhibit overoxidation of the desired products. In particular significant concentrations of ring-opened by products including 6-hydroxyhexanoic acid and glutaric acid are produced at even moderate rates of conversion [5, 6]. Typically, KA oil production involves two consecutive steps: (i) the non-catalytic auto-oxidation of cyclohexane to cyclohexyl hydroperoxide (CHHP) and (ii) the catalysed decomposition of CHHP to KA oil, with carboxylic acids and esters also produced in low quantities.

The high energy costs that result from the use of elevated temperatures and the difficulties associated with separating homogeneous catalysts from the product stream has led to growing interest in the use of heterogeneous catalysts for aerobic KA oil production, with previous studies reporting the efficacy of transition metal containing molecular sieves [7–10] and precious metals catalyst [11, 12]. While further studies have reported that the replacement of molecular O₂ with either tert-butylhydroperoxide (TBHP) [13, 14] or pre-formed H₂O₂ [15, 16] allows for the use of significantly lower reaction temperatures. However, typically these oxidants are utilised in excess to improve efficiency [14], with the catalysed and non-catalysed decomposition of H₂O₂ to H₂O a major competitive reaction pathway.

Apart from concerns around atom efficiency there are several economic and environmental drawbacks associated with the use of commercial H₂O₂ as an oxidant. These are generally associated with the means by which H₂O₂ is produced on an industrial scale, the in-direct or anthraquinone oxidation (AO) process, which although highly optimized, with high H₂ selectivity, is only economically viable when operating on a large scale, often prohibiting production at the site of final use. As such H₂O₂ is typically transported and stored, at concentrations in excess of 70 wt.% prior to dilution, effectively wasting significant amounts of energy utilised in concentration. Furthermore, the low stability of H₂O₂ at mild temperatures necessitates the use of acidic stabilizers to prevent decomposition to H₂O during transport and storage, these stabilising agents often need to be removed from product streams prior to shipping, with additional costs passed on to the end user [17, 18].

The in-situ production of H₂O₂ from molecular H₂ and O₂ would offer an attractive alternative to the use of pre-formed H₂O₂ as an oxidant for cyclohexane, overcoming the aforementioned issues associated with commercial H₂O₂. In addition, in-situ H₂O₂ production would also lead to significantly reduced process costs, compared to the current industrial route to KA oil, associated with lower reaction temperatures. Indeed we have recently demonstrated that limited concentrations of

KA oil can be produced via the in-situ production of H₂O₂ over supported AuPd nanoparticles, prepared via a conventional wet-impregnation procedure, under reaction conditions where no conversion of cyclohexane is observed using O₂ alone [19, 20].

With these previous studies in mind we now investigate a range of bi-functional Pd-based catalysts that combine the H₂O₂ synthesising activity of Pd and the ability of a range of transition metals to selectively catalyse the oxidation of cyclohexane to KA oil.

2 Experimental

2.1 Catalyst Preparation

Mono- and bi-metallic 1%PdX/TiO₂ (X = Au, Mn, Fe, V, Co, Ni, Cu, Ce) catalysts, prepared on a weight basis, with a Pd: X ratio of 1: 1 (wt/wt) have been synthesised via a modified impregnation procedure, based on methodology previously reported in the literature [21, 22]. With catalysts produced via an impregnation procedure widely studied for both the direct synthesis of H₂O₂ [23] and cyclohexane oxidation [24] due to the simplicity and ease with which this approach can be scaled to meet industrial application. The procedure to produce 0.5% Au–0.5% Pd/TiO₂ (2 g) is detailed below, with a similar methodology utilized for all mono- and bi-metallic catalysts using chloride based metal precursors in all cases (see Table S.1 for further details). In all cases catalysts have been prepared using PdCl₂ (0.58 M HCl, 6 mgmL⁻¹, Sigma-Aldrich).

Aqueous acidified PdCl₂ solution (1.667 mL, 0.58 M HCl, 6 mgmL⁻¹, Sigma-Aldrich) and aqueous HAuCl₄·3H₂O solution (0.8263 mL, 12.25 mgmL⁻¹, Strem Chemicals) were mixed in a 50 mL round-bottom flask and heated to 65 °C with stirring (1000 rpm) in a thermostatically controlled oil bath, with total volume fixed to 16 mL using H₂O (HPLC grade). Upon reaching 65 °C, TiO₂ (1.98 g, Degussa, P25) was added over the course of 5 min with constant stirring. The resulting slurry was stirred at 65 °C for a further 15 min, following this the temperature was raised to 95 °C for 16 h to allow for complete evaporation of water. The resulting solid was ground prior to a reductive heat treatment (5%H₂/Ar, 500 °C, 4 h, 10 °C min⁻¹).

Surface area measurements for key materials, as determined by 5-point N₂ adsorption, are reported in Table S2.

2.2 Catalyst Testing

2.2.1 Note 1

Reaction conditions used within this study operate below the flammability limits of gaseous mixtures of H₂ and O₂ (4–94%).

2.2.2 Note 2

The conditions used within this work for H₂O₂ synthesis and degradation have previously been investigated, with the presence of CO₂ as a diluent for reactant gases and a methanol co-solvent have identified as key to maintaining high catalytic efficacy towards H₂O₂ production [22, 25].

2.3 Direct Synthesis of H₂O₂ From H₂ and O₂

Hydrogen peroxide synthesis was evaluated using a Parr Instruments stainless steel autoclave with a nominal volume of 50 mL, equipped with a PTFE liner and a maximum working pressure of 2000 psi. To test each catalyst for H₂O₂ synthesis, the autoclave liner was charged with catalyst (0.01 g) and HPLC grade standard solvents (5.6 g methanol and 2.9 g H₂O). The charged autoclave was then purged three times with 5% H₂ / CO₂ (100 psi) before filling with 5% H₂ / CO₂ to a pressure of 420 psi, followed by the addition of 25% O₂ / CO₂ (160 psi) to achieve a total pressure of 580 psi. Pressures of 5% H₂ / CO₂ and 25% O₂ / CO₂ are given as gauge pressures. The reaction was conducted at a temperature of 20 °C, for 0.5 h with stirring (1200 rpm), with the reactor temperature controlled using a HAAKE K50 bath/circulator using an appropriate coolant.

H₂O₂ productivity was determined by titrating aliquots of the final solution after reaction with acidified Ce(SO₄)₂ (0.0085 M) in the presence of ferroin indicator. Catalyst productivities are reported as mol_{H₂O₂}kg_{cat}⁻¹ h⁻¹.

2.4 Degradation of H₂O₂

Catalytic activity towards H₂O₂ degradation was determined in a similar manner to that used to measure the direct synthesis activity of a catalyst. The autoclave liner was charged with methanol (5.6 g, HPLC standard), H₂O₂ (50 wt. %, 0.69 g), H₂O (2.21 g, HPLC standard) and catalyst (0.01 g), with the solvent composition equivalent to a 4 wt. % H₂O₂ solution. From the solution, prior to the addition of the catalyst, two 0.05 g aliquots were removed and titrated with acidified Ce(SO₄)₂ solution using ferroin as an indicator to determine an accurate concentration of H₂O₂ at the start of the reaction. The autoclave was purged three times with 5% H₂ / CO₂ (100 psi) before filling with 5% H₂ / CO₂ to a gauge pressure of 420 psi. The reaction was conducted at

a temperature of 20 °C, for 0.5 h with stirring (1200 rpm). After the reaction was complete the catalyst was removed from the reaction mixture by filtration and two 0.05 g aliquots were titrated against the acidified Ce(SO₄)₂ solution using ferroin as an indicator. The degradation activity is reported as mol_{H₂O₂}kg_{cat}⁻¹ h⁻¹.

2.5 Cyclohexane Oxidation via the In-situ Production of H₂O₂

The conditions utilised within this work have previously been optimised for the oxidation of cyclohexane via in-situ H₂O₂ production [19].

Cyclohexane oxidation has been evaluated using a Parr Instruments stainless steel autoclave with a nominal volume of 50 mL, equipped with a PTFE liner and a maximum working pressure of 2000 psi. To test each catalyst for cyclohexane oxidation, the autoclave was charged with catalyst (0.05 g), t-butanol solvent (6.375 g, Sigma Aldrich) and cyclohexane (2.125 g, 25 mmol, Sigma Aldrich) with mesitylene (0.43 g, 3.6 mmol, Sigma Aldrich) used as an internal standard. The charged autoclave was then purged three times with 5% H₂/N₂ (100 psi) before filling with 5% H₂/N₂ (420 psi, 2.5 mmol H₂) followed by the addition of 25% O₂/N₂ (160 psi, 4.8 mmol O₂) to achieve a total pressure of 580 psi. With all pressures given as gauge pressure. The temperature was then increased to 80 °C with stirring (500 rpm). Once the desired temperature was reached the reaction mixture was stirred (1200 rpm) for 17 h. After the reaction was complete the reactor was cooled in ice to a temperature of 15 °C, upon which a gas sample was taken for analysis by gas chromatography, using a Varian CP-3380 equipped with a TCD detector and a Porapak Q column. Product yield was determined by gas chromatography using a Varian 3200 GC equipped with a FID and CP Wax 42 column.

Quantification of the intermediate cyclohexyl hydroperoxide (CHHP) is determined by reacting a 2 mL aliquot of the post reaction mixture with an excess of triphenyl phosphine (0.13 g, 0.5 mmol). Reaction of triphenyl phosphine and CHHP produces cyclohexanol and hence comparison of GC analysis for cyclohexanol pre- and post-treatment with triphenyl phosphine can determine the yield of CHHP.

Catalytic conversion of H₂ was determined using a Varian 3800 GC fitted with TCD and equipped with a Porapak Q column.

H₂ conversion (Eq. 1), cyclohexane conversion (Eq. 2) and selectivity to all C₆ products based on H₂ (Eq. 3) are defined as follows:

$$\text{H}_2\text{Conversion (\%)} = \frac{\text{mmol}_{\text{H}_2(t(0))} - \text{mmol}_{\text{H}_2(t(1))}}{\text{mmol}_{\text{H}_2(t(0))}} \times 100 \quad (1)$$

$$\text{Cyclohexane Conversion (\%)} = \frac{\text{mmol}_{\text{Cyclo}}(t(0)) - \text{mmol}_{\text{Cyclo}}(t(1))}{\text{mmol}_{\text{Cyclo}}(t(0))} \times 100 \quad (2)$$

$$\text{C}_6\text{Product Selectivity (\%)} = \frac{\text{Total product (mmol)}}{\text{H}_2 \text{ conversion (mmol)}} \times 100 \quad (3)$$

2.5.1 Note 3

Given the relatively low conversion rates observed within this work total product yield (including CHHP, cyclohexanone and cyclohexanol) is used as a substitute for cyclohexane conversion.

2.6 Hot-Filtration Experiments

In order to determine the contribution of leached species towards the oxidation of cyclohexane, a standard reaction is carried out to that described above. After the initial 17 h reaction the heterogeneous catalyst was removed via filtration and the reaction solution returned to the autoclave, for a further 17 h reaction, under the conditions outlined above.

2.7 Catalyst Reusability in the Oxidation of Cyclohexane via In-situ Production of H₂O₂

In order to determine catalyst reusability, a similar procedure to that outlined above for the oxidation of cyclohexane is followed utilising 0.15 g of catalyst. Following the initial test, the catalyst was recovered by filtration, washed with cyclohexane, and dried (30 °C, 17 h, under vacuum); from the recovered catalyst sample 0.05 g was used to conduct a standard cyclohexane oxidation experiment.

2.8 Cyclohexane Oxidation Under Aerobic Conditions

To evaluate the efficacy of in-situ conditions (H₂ + O₂) catalysts have also been studied for their activity towards cyclohexane oxidation under aerobic conditions. A procedure similar to that outlined above for the oxidation of cyclohexane is followed using 25%O₂/N₂ (160 psi) and N₂ (420 psi) to maintain total reaction pressure at 580 psi.

2.9 Catalyst Characterisation

A Thermo Scientific K-Alpha⁺ photoelectron spectrometer was used to collect XP spectra utilising a micro-focused monochromatic Al K_α X-ray source operating at 72 W. Data was collected over an elliptical area of approximately 400 μm² at pass energies of 40 and 150 eV for

high-resolution and survey spectra, respectively. Sample charging effects were minimised through a combination of low energy electrons and Ar⁺ ions, consequently this resulted in a C(1 s) line at 284.8 eV for all samples. All data was processed using CasaXPS v2.3.24 using a Shirley background, Scofield sensitivity factors [26] and an electron energy dependence of −0.6 as recommended by the manufacturer.

Scanning Transmission Electron Microscopy (STEM) and X-ray Energy Dispersive Spectroscopy (X-EDS) data was taken using a JEOL JEM-ARM200CF microscope in Diamond Laboratory. The TEM specimens investigated were the as-prepared 0.5%Pd-0.5%V/TiO₂ catalyst and the analogous sample after use in the cyclohexane oxidation reaction.

Total metal leaching from the supported catalyst was quantified via inductively coupled plasma mass spectrometry (ICP-MS). Post-reaction solutions were analysed using an Agilent 7900 ICP-MS equipped with I-AS auto-sampler. All samples were diluted by a factor of 10 using HPLC grade H₂O (1% HNO₃ and 0.5% HCl matrix). All calibrants were matrix matched and measured against a five-point calibration using certified reference materials purchased from Perkin Elmer and certified internal standards acquired from Agilent.

Brunauer Emmett Teller (BET) surface area measurements were conducted using a Quadrasorb surface area analyser. A 5-point isotherm of each material was measured using N₂ as the adsorbate gas. Samples were degassed at 250 °C for 2 h prior to the surface area being determined by 5-point N₂ adsorption at −196 °C, and data analysed using the BET method.

3 Results and Discussion

Our initial studies investigated the efficacy of a series of mono-metallic catalysts, prepared by a modified impregnation procedure, towards the direct synthesis and subsequent degradation of H₂O₂, under conditions favourable towards H₂O₂ stability (Figure S.1) [22, 25]. The limited activity towards both the formation and subsequent degradation of H₂O₂ is clear for all mono-metallic catalysts with the exception of the 1% Pd/TiO₂ catalyst, which displays rates of H₂O₂ synthesis (30 mol_{H₂O₂}kg_{cat}^{−1} h^{−1}) and H₂O₂ degradation (198 mol_{H₂O₂}kg_{cat}^{−1} h^{−1}) far greater than those observed for the non-Pd analogues. The greater activity of the 1%Pd/TiO₂ catalyst is perhaps unsurprising given the extensive studies into supported Pd catalysts for H₂O₂ direct synthesis [27, 28]. The alloying of Pd with Au has been widely reported to enhance catalytic activity towards the direct synthesis of H₂O₂ with the synergistic enhancement observed for AuPd alloys typically attributed to electronic and isolation effects [29–32]. In keeping with these studies, we report a significant improvement in catalytic activity towards

H₂O₂ synthesis over the 0.5% Au-0.5% Pd/TiO₂ catalyst (68 mol_{H₂O₂} kg_{cat}⁻¹ h⁻¹). However, we do not observe a decrease in H₂O₂ degradation rate, which is typically reported upon the alloying of Au and Pd [33]. With this observation in keeping with the findings of Santos et al. who have recently investigated a series of AuPd catalysts, prepared by an identical procedure, for H₂O₂ synthesis, under a range of reaction conditions [22]. This is likely due to the use of a reductive heat treatment in the preparation of these catalysts and the resulting formation of homogeneous alloy nanoparticles [21]. With numerous studies reporting the formation of a Au-core PdO-shell nanoparticle morphology, promoted by the oxidative heat treatment of AuPd catalysts, to be crucial to their enhanced selectivity towards H₂O₂ [25, 34].

In recent years focus has shifted towards alloying Pd with a range of non-precious metals, with numerous studies reporting the enhanced catalytic efficacy achieved through the introduction of Sn [35, 36], Ag [37], Zn [38], Ni [39, 40], In [41, 42], Sb [43], and Te [44] into Pd nanoparticles. Typically, the improved selectivity of the bimetallic catalysts has been attributed to a combination of a reduction of contiguous Pd ensembles and a modification of Pd oxidation state. In keeping with these previous reports our investigations also demonstrate the enhanced catalytic efficacy that can be achieved through the introduction of a range of transition metals into supported Pd catalyst (Fig. 1), with a clear reduction in H₂O₂ degradation rate observed upon the introduction of all secondary metals, with the exception of Au. This is perhaps unexpected given the ability of a range of these secondary metals, such as Fe, Mn and Cu, to catalyse the decomposition of H₂O₂ through Fenton or Fenton-like pathways [45, 46]. However, it is possible that the limited degradation activity observed can be related to a combination of two factors (i) the choice of reaction conditions used to evaluate H₂O₂ synthesis activity, with the *in-situ* formation of carbonic acid, through the dissolution of the CO₂ reactant gas diluent resulting in the stabilisation of H₂O₂ and (ii) the modification of Pd oxidation states upon introduction of secondary metals, as observed via XPS analysis (Table S.3), with the formation of mixed domains of Pd⁰-Pd²⁺ reported to offer enhanced catalytic efficacy in both H₂O₂ synthesis [47, 48] and aerobic oxidation reactions [49]. It should be noted that our analysis by XPS reveals that the introduction of Au, unlike the majority of the other transition metals, does not promote the formation of these mixed oxidation state domains, which may explain the enhanced rates of H₂O₂ synthesis and degradation observed over this catalyst [50].

Building on these findings we next investigated the efficacy of these Pd-based bi-metallic catalysts towards the selective oxidation of cyclohexane (Fig. 2). It should be noted that under the reaction conditions used within this study no residual H₂O₂ was measured in post reaction

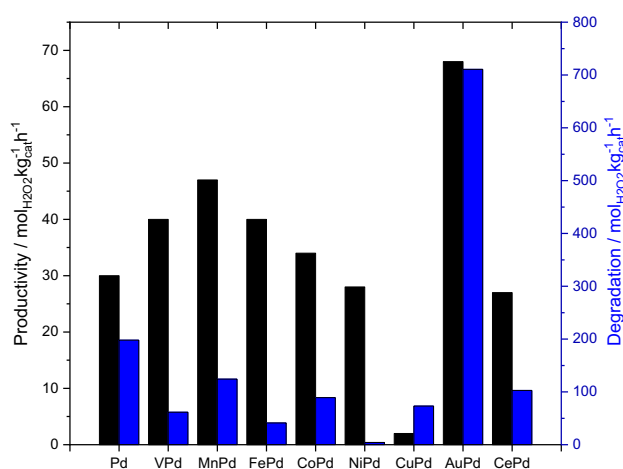


Fig. 1 Catalytic activity of bimetallic supported catalysts towards the direct synthesis (Black bars) and degradation of H₂O₂ (Blue bars). H₂O₂ direct synthesis reaction conditions: Catalyst (0.01 g), H₂O (2.9 g), MeOH (5.6 g), 5% H₂/CO₂ (420 psi), 25% O₂/CO₂ (160 psi), 0.5 h, 20 °C, 1200 rpm. H₂O₂ degradation reaction conditions: Catalyst (0.01 g), H₂O₂ (50 wt.% 0.68 g) H₂O (2.22 g), MeOH (5.6 g), 5% H₂/CO₂ (420 psi), 0.5 h, 20 °C, 1200 rpm

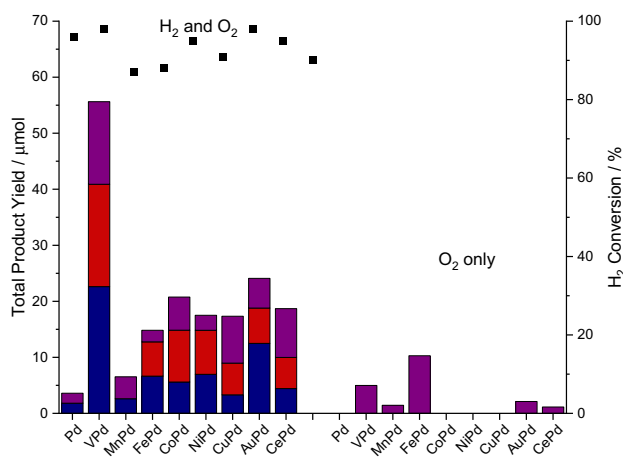


Fig. 2 Catalytic activity of bi-metallic Pd based supported catalysts towards the oxidation of cyclohexane via the in-situ production of H₂O₂. Cyclohexanol; blue, cyclohexanone; red, CHHP; purple. Reaction conditions: Catalyst (0.05 g), cyclohexane (2.13 g, 25 mmol), t-butanol (6.37 g), 5% H₂ / N₂ (420 psi), 25% O₂ / N₂ (160 psi), 17 h, 80 °C 1200 rpm. Note: When under aerobic conditions 25% O₂ / N₂ (160 psi) is used in addition to N₂ (420 psi) to maintain total pressure. All other conditions as described above

solutions. This is unsurprising given the comparatively high reaction temperatures and long reaction times utilised within this work. However, our previous studies, have elucidated the ability of H₂O₂ to be synthesised under similar reaction conditions, although this previous study reported complete selectivity towards cyclohexanol, likely as a result of the short reaction times utilised [20].

Interestingly the introduction of a range of secondary metals into supported Pd nanoparticles is seen to lead to a significant increase in catalytic activity towards the oxidation of cyclohexane under in-situ conditions (i.e. in the presence of H_2 and O_2). As expected, given the extensive studies into AuPd systems for a range of selective oxidation reactions [51–53] as well as for the direct synthesis of H_2O_2 [54, 55], in this study the introduction of Au into a supported Pd catalyst is also seen to result in an enhancement in the oxidation of cyclohexane, with a total C_6 product yield of 24.1 μmol observed over the 0.5%Au-0.5%Pd/ TiO_2 catalyst, far greater than that observed over the Pd-only analogue (3.6 μmol), with the former also displaying a significantly enhanced selectivity to all C_6 products compared to the 1%Pd/ TiO_2 catalyst (Table S.4).

It should also be noted that the total product yield, observed over the 0.5%Au-0.5%Pd/ TiO_2 catalyst studied within this work (prepared via a modified-impregnation methodology) is far greater than that we recently reported for an analogous catalyst prepared via a conventional wet co-impregnation methodology (13 μmol) [19]. With this ascribed, at least in part, to the greater activity of the catalyst synthesised via a modified-impregnation methodology to synthesise H_2O_2 , as indicated by our testing under conditions conducive towards H_2O_2 (Table S.5).

Interestingly, despite demonstrating a limited activity towards H_2O_2 synthesis (40 $\text{mol } H_2O_2/\text{kg}_{\text{cat}}^{-1} \text{ h}^{-1}$), the 0.5%V-0.5%Pd/ TiO_2 catalyst is observed to display a total C_6 product yield (56 μmol) far greater than that of either the 0.5%Au-0.5%Pd/ TiO_2 (24.1 μmol), or 1%Pd/ TiO_2 (3.6 μmol) catalysts (Fig. 2). With a corresponding improvement in selectivity towards all C_6 products based on H_2 also observed over the 0.5%V-0.5%Pd/ TiO_2 catalyst (Table S.4). Evaluation of apparent turnover frequencies (TOFs) based on total metal content further highlights the improved activity of the 0.5%V-0.5%Pd/ TiO_2 catalyst compared to all other bi-metallic catalysts studied (Table S.6).

The high activity of V-based catalysts when used in conjunction with pre-formed H_2O_2 to catalyse the oxidation of alkanes has been widely linked to the V^{4+}/V^{5+} redox cycle [56–59]. With the enhanced activity of the VPd supported catalyst in this work attributed to the dual functionality of

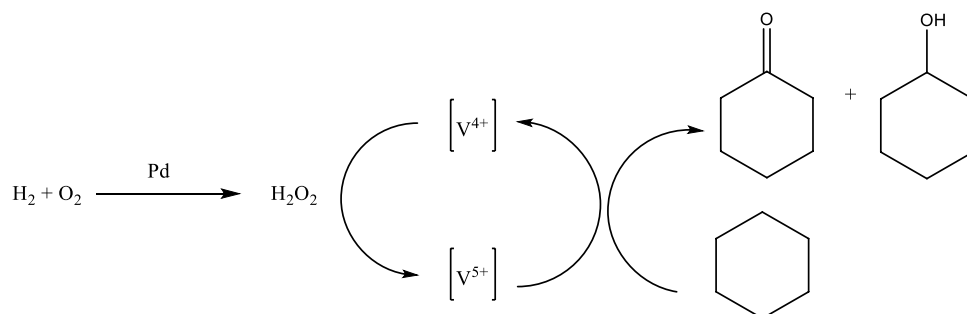
the catalyst, with Pd catalysing the synthesis of H_2O_2 , which is then subsequently activated by V (Scheme 1). Indeed a similar explanation can be attributed to the enhanced activity observed when alloying Pd with Fe (14.8 μmol) or other Fenton-like metals used in this study such as Cu, (18.7 μmol) with previous studies reporting the high cyclohexane oxidation activity when using a range of Fenton-like metals in conjunction with pre-formed H_2O_2 [16, 60].

As expected, given the relatively low reaction temperatures used within this work the activity of all catalysts under in-situ reaction conditions (i.e. in the presence of H_2 and O_2) greatly outperforms that observed using O_2 alone, clearly highlighting the benefits of the in-situ approach (Fig. 2). Indeed, under in-situ reaction conditions the 0.5%V-0.5%Pd/ TiO_2 catalyst is seen to offer greater product yield (56 μmol) than that observed when using commercial H_2O_2 (25.9 μmol) (Figure S.2).

Further studies reveal the benefits of immobilising both Pd and V onto the same grain of support (Fig. 3a). The combination of the monometallic 1%Pd/ TiO_2 and 1%V/ TiO_2 catalysts as a physical mixture, is seen to result in a marked improvement in total product yield (31.8 μmol) and selectivity to all C_6 products based on H_2 (Table S.7) compared to the corresponding monometallic catalysts. However, both the total product yield and selectivity towards C_6 products observed over the physical mixture system is still far lower than that observed over the bimetallic catalyst. The activity of the 1%V/ TiO_2 catalyst when used alone (17.8 μmol) is noteworthy and can be ascribed to the catalysed aerobic oxidation pathway, with V catalysts well reported to offer some activity towards cyclohexane oxidation, even at ambient temperatures [61]. It should be noted that in the case of the 1%V/ TiO_2 catalyst the extent of H_2 conversion was so low to be within experimental error, further supporting the role of V to catalyse the aerobic route.

The excellent efficacy of V based catalysts towards the oxidation of alkanes, either in the form of unsupported vanadium oxides [62] or vanadium oxides supported on secondary oxide supports [63, 64] is well known, with perhaps the greatest interest placed on the vanadium phosphorus oxide (VPO) catalysts [58, 59, 65, 66]. With these studies in mind, we next compared the efficacy of the 0.5%V-0.5%Pd/ TiO_2

Scheme 1 Proposed reaction pathway for the selective oxidation of cyclohexane via in-situ H_2O_2 production



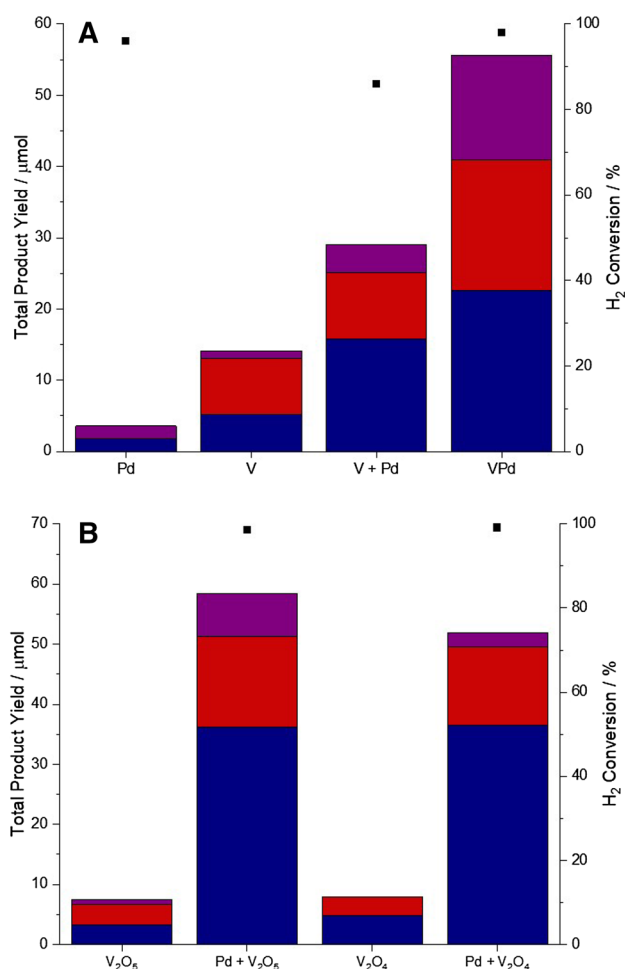


Fig. 3 **a** Catalytic performance of V-Pd catalysts towards the oxidation of cyclohexane via the in-situ production of H₂O₂. **b** The activity of 1% Pd/TiO₂, 1% VPd/TiO₂, V₂O₅, V₂O₄, and physical mixtures of 1% Pd/TiO₂ and vanadium oxides towards the oxidation of cyclohexane via the in-situ production of H₂O₂. Cyclohexanol; blue, cyclohexanone; red, CHHP; purple. Reaction conditions: Catalyst (0.05 g), cyclohexane (2.13 g, 25 mmol), t-butanol (6.37 g), 5% H₂ / N₂ (420 psi), 25% O₂ / N₂ (160 psi), 17 h, 80 °C 1200 rpm. Note: Where physical mixtures have been used 0.025 g of each catalyst are utilised

catalyst with a physical mixture of vanadium oxides (V₂O₄ and V₂O₅) and a 1%Pd/TiO₂ catalyst (Fig. 3b). In keeping with the background aerobic activity observed over the 1%V/TiO₂ catalyst, we observe some activity when using either V₂O₄ (7.9 μmol) or V₂O₅ (7.4 μmol) alone, again with negligible conversion of H₂ observed. When using the 1%Pd/TiO₂ catalyst in addition with either vanadium oxide a significant improvement in catalytic activity and selectivity to all C₆ products based on H₂ is seen, compared to when either component is used in isolation (Table S.8). The activity and H₂ selectivity of the physical mixtures of vanadium oxide and 1%Pd/TiO₂ are comparable to that observed for the 0.5%V-0.5%Pd/TiO₂ catalyst despite the far lower concentrations of both Pd and V present in the bi-metallic

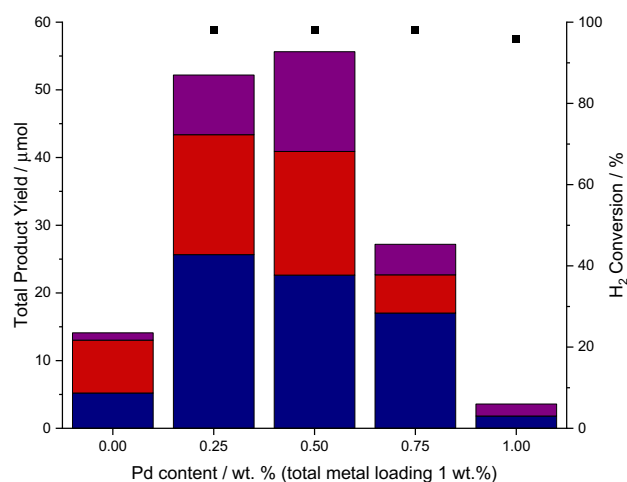


Fig. 4 Catalytic activity of bi-metallic 1%VPd/TiO₂ supported catalysts towards the oxidation of cyclohexane via the in-situ production of H₂O₂. Cyclohexanol; blue, cyclohexanone; red, CHHP; purple. Reaction conditions: Catalyst (0.05 g), cyclohexane (2.13 g, 25 mmol), t-butanol (6.37 g), 5% H₂ / N₂ (420 psi), 25% O₂ / N₂ (160 psi), 17 h, 80 °C 1200 rpm

catalyst, further supporting the need for both metals to be present on the same grain of support in order to reach maximal efficiency.

With the high catalytic efficacy of Pd-V/TiO₂ catalysts established we next investigated the effect of V: Pd ratio, while maintaining total metal loading at 1 wt.% (Fig. 4). Given the separate and distinct roles of Pd and V, with the former primarily catalysing the synthesis of H₂O₂, and the latter subsequently activating the synthesised H₂O₂ and catalysing the oxidation of cyclohexane it is imperative to balance both reactions to achieve maximal oxidant efficiency. An optimal catalyst formulation of 0.5%V-0.5%Pd/TiO₂ is observed, with this catalyst displaying the greatest total product yield and selectivity to all C₆ products (Table S.9) and highest turnover frequency (Table S.10).

The oxidation state of Pd is well known to dictate catalytic activity towards the direct synthesis and subsequent degradation of H₂O₂, with the enhanced activity of reduced Pd-species towards both H₂O₂ formation and degradation to water (via decomposition and hydrogenation pathways) compared to analogous Pd²⁺ catalysts widely reported [47, 50, 67]. Recently several studies have revealed the improved efficacy of mixed domains of Pd⁰-Pd²⁺ towards both H₂O₂ synthesis [47, 48] and a range of aerobic oxidation transformations [49]. Likewise, the oxidation state of V is a crucial factor in the oxidation of cyclohexane, with a general agreement in the literature that the V⁴⁺/V⁵⁺ redox cycle is crucial in achieving high efficacy, while the accumulation of V³⁺ is suggested to lead to deactivation of the catalyst [65, 68].

XPS spectra of the as-prepared 1%VPd/TiO₂ catalysts, with varying V: Pd ratios can be seen in Fig. 5. Upon

co-immobilisation of both metals onto the same grain of support a stark difference in both Pd and V oxidation states is observed, compared to those present in the corresponding monometallic analogues.

With the introduction of V into a Pd-only catalyst the proportion of Pd²⁺ present is seen to increase considerably compared to the 1%Pd/TiO₂ analogue, which consists almost entirely of Pd⁰. Indeed, this culminates in a total shift towards Pd²⁺ in the case of the 0.75%V-0.25%Pd/TiO₂ catalyst (Fig. 5d). However, this is not seen to detrimentally affect catalytic performance, and indeed it is likely that the oxidation states of the fresh material will not be representative of that under-reaction conditions.

For all catalysts containing V, two oxidation states of V are noted at 517.2 and 516.1 eV representative of V⁵⁺ and V⁴⁺ species respectively.[69] Notably, for the 0.25%V-0.75%Pd/TiO₂ catalyst, a shift towards a lower binding energy, *ca.* 515.5 eV, is observed (Fig. 5h) which is typically representative of V³⁺ oxides and hydroxides. This coincides with a stark loss in catalytic performance (Fig. 4, Table S.9) and is in keeping with previous studies, which report that the presence of V³⁺ is able to inhibit the activity of V-based catalysts towards cyclohexane oxidation [65, 68].

For any heterogeneous catalyst operating in a three-phase system the possibility of the leaching of the active phase and resulting homogeneous contribution to observed catalytic performance is of great concern, with the activity of homogeneous V and Pd species known to catalyse the oxidation of cyclohexane and the direct synthesis of H₂O₂ respectively [70, 71]. Analysis of post reaction solutions via ICP-MS (Table S.11) reveals minimal leaching of Pd, with approximately 0.29% (0.001 wt.%) Pd detected in the post-reaction solution, on the other hand a significant amount of leached V is observed, approximately 21% (0.11 wt.% V).

Subsequent experiments, using an identical number of moles of V to that present in the 0.5%V-0.5%Pd/TiO₂ catalyst, further identify the ability of homogeneous V species (as VCl₃) to catalyse the oxidation of cyclohexane (11.7 μmol), though aerobic pathways as indicated by the negligible H₂ conversion observed. In keeping with our earlier studies (Fig. 3a–b) a significant improvement in catalytic performance is seen when combining VCl₃ with a heterogeneous Pd catalyst (33 μmol), again so that total moles of metal are identical to that present in the 0.5%V-0.5%Pd/TiO₂ catalyst (Figure S.3, Table S.12). However, as in these earlier studies the 0.5%V-0.5%Pd/TiO₂ catalyst is seen to offer

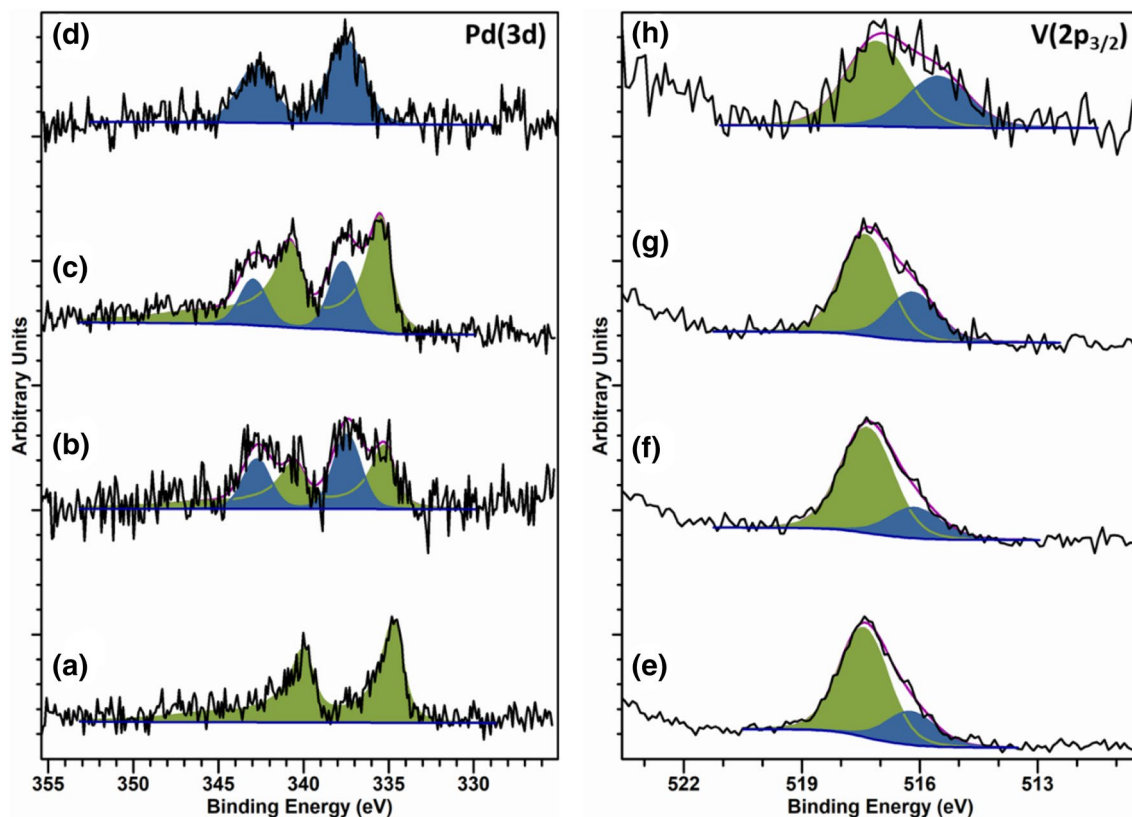


Fig. 5 Pd(3d) and V(2p_{3/2}) core levels spectra for: (a) 1%Pd/TiO₂, (b & h) 0.25%V-0.75%Pd/TiO₂, (c & g) 0.5%V-0.5%Pd/TiO₂, (d & f) 0.75%V-0.25%Pd/TiO₂ and (e) 1%V/TiO₂. For Pd (3d) region: Pd⁰ (Green) Pd²⁺ (Blue), for V(2p_{3/2}) region: V⁵⁺ (Green), V⁴⁺ (Blue)

greater product yield (56 μmol), highlighting the need for both metals to be in close proximity.

Hot filtration experiments (Fig. 6) confirm a contribution to cyclohexane oxidation from leached species (31.8 μmol). However, the contribution to total observed products in the hot filtration experiment from the decomposition of existing CHHP (i.e. CHHP produced in the presence of the heterogeneous catalyst) should be considered, with 14 μmol CHHP detected in the heterogeneously catalysed reaction, prior to the hot filtration experiment. Given the high stability of Pd, with minimal leaching observed in post reaction solutions, it is reasonable to assume that the major route to KA oil in the hot filtration experiments, excluding the decomposition of the pre-formed CHHP (which possibly accounts for more than 40% of the additional observed products), is via V catalysed aerobic oxidation pathways, as previously observed when using homogeneous V species, vanadium oxides or 1%V/TiO₂ as catalysts for the cyclohexane oxidation reaction (Fig. 3, Figure S.3).

Despite the extensive leaching of V a significant improvement in the activity of the 0.5%V-0.5%Pd/TiO₂ catalyst is seen upon re-use, (90.9 μmol) (Fig. 6) with a subsequent improvement in catalytic selectivity based on H₂ also observed (Table S.13). While we have established that the activity may in part be attributed to leached V species, with a continual leaching of V observed upon re-use (14%, 0.07 wt.% V), there is clearly a significant heterogenous component to the oxidation reaction.

Evaluation of the fresh and used 0.5%V-0.5%Pd/TiO₂ catalysts by XPS (Figure S.4, Table S.14) reveals a shift in both Pd(3d) and V(2p) spectra indicative of an increase in both Pd²⁺ and V⁴⁺ content, with no V³⁺ observed. This in turn correlates well with a measurable improvement in

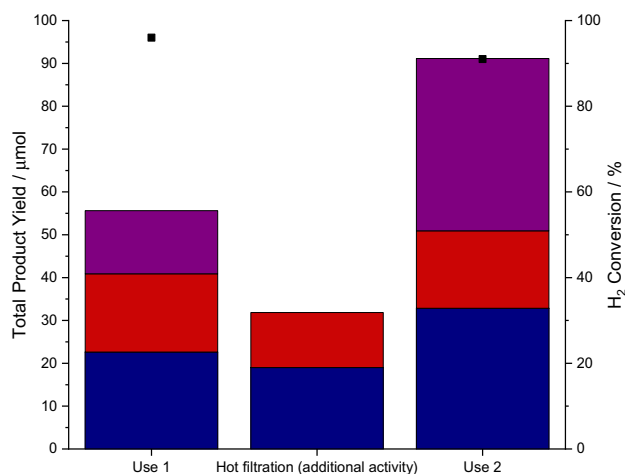


Fig. 6 Reusability of 0.5%V-0.5%Pd/TiO₂ in the oxidation of cyclohexane via the in-situ production of H₂O₂. Cyclohexanol; blue, cyclohexanone; red, CHHP; purple. Reaction conditions: Catalyst (0.05 g), cyclohexane (2.13 g, 25 mmol), t-butanol (6.37 g), 5% H₂ / N₂ (420 psi), 25% O₂ / N₂ (160 psi), 17 h, 80 °C 1200 rpm

both catalytic performance and selectivity based on H₂ (Fig. 6, Table S.11), which is perhaps unsurprising, with the formation of mixed domains of Pd⁰-Pd²⁺ reported to offer enhanced catalytic efficacy in both H₂O₂ formation and aerobic oxidation reactions [48, 49].

Meanwhile analysis of the as-prepared 0.5%V-0.5%Pd/TiO₂ catalyst, (Fig. 7a) in addition to the analogous sample after use in the cyclohexane oxidation reaction (Fig. 7b) by HAADF-STEM can be seen in Fig. 7, with accompanying EDX analysis reported in Figure S.5. From our analysis there is no clear indication of alloyed Pd-V species within the fresh sample, with V observed to be highly dispersed over the entirety of the support, whereas Pd is present as discrete nanoparticles. In keeping with previous investigations these Pd nanoparticles are generally relatively small (2–5 nm) with very few larger agglomerates (> 10 nm) observed [22]. Although it should be noted that it was not possible to count a statistically relevant number of nanoparticles to generate an accurate mean particle size for the fresh and used catalysts. As with the fresh sample, analysis of the 0.5%V-0.5%Pd/TiO₂ catalyst after use in the cyclohexane oxidation reaction indicates that V remains well dispersed, although it should be reiterated that our analysis by ICP-MS (Table S.11) does indicate leaching of V during the reaction, with these homogeneous species only responsible for limited catalytic activity.

By comparison to V, some agglomeration of the Pd nanoparticles is observed upon use in the cyclohexane oxidation reaction, with an increased proportion of Pd present as larger (> 10 nm) nanoparticles, although the smaller species previously observed in the fresh sample are still present. This is in keeping with our previous investigation into the ability of supported AuPd nanoparticles to catalyse the oxidation of cyclohexane under identical reaction conditions [19]. As in this previous study the apparent increase in particle size does not appear to detrimentally effect catalytic efficacy towards cyclohexane upon re-use (Fig. 6).

4 Conclusion

We have demonstrated that it is possible to achieve appreciable rates of cyclohexane oxidation to KA oil using H₂O₂ generated in-situ using a 1%VPd/TiO₂ catalyst, prepared by a readily scalable modified-impregnation procedure. This is observed using conditions where activity is limited when using molecular O₂ alone, with no loss in catalytic activity observed with re-use, although catalyst stability is still of concern. The enhanced performance of the optimal 0.5%V-0.5%Pd/TiO₂ catalyst, observed to be an order of magnitude greater than that of the Pd-only analogue, is attributed to the production of domains of mixed Pd

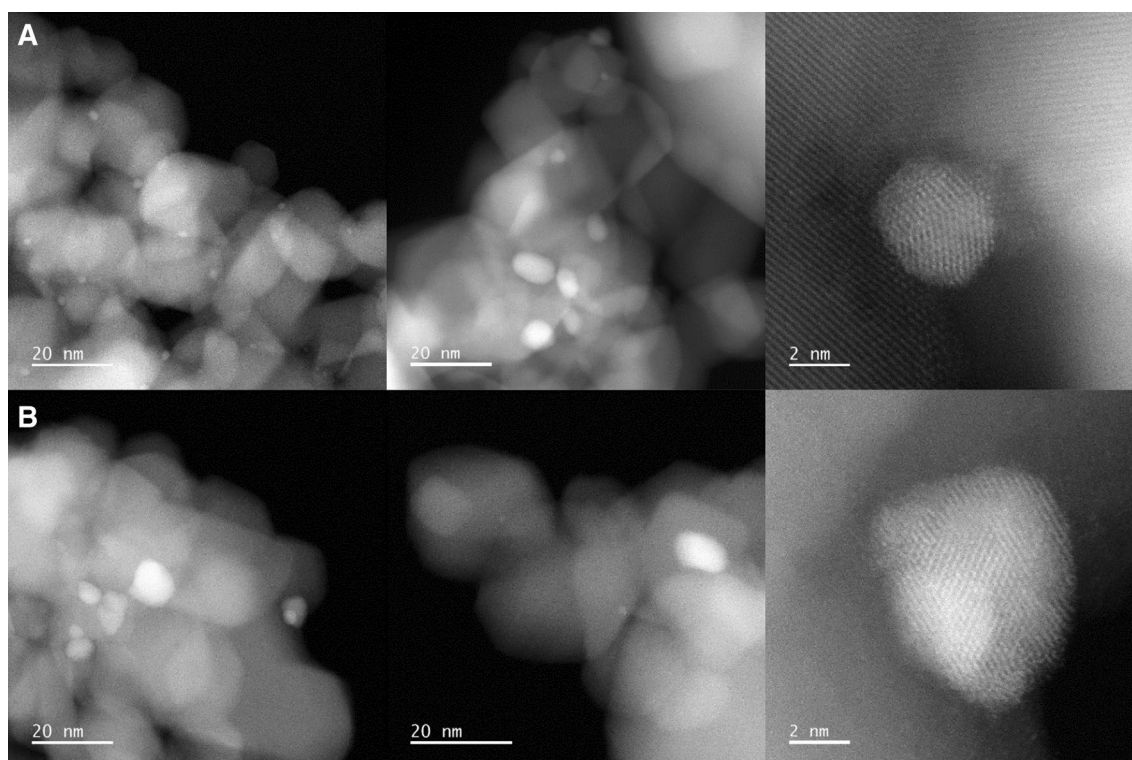


Fig. 7 Representative bright field transmission electron micrographs of 0.5%V-0.5%Pd/TiO₂ catalyst **a** as prepared by modified impregnation methodology and **b** after use in the cyclohexane oxidation reaction, under in-situ conditions

oxidation states upon V incorporation and the dual functionality of the catalyst. We consider that these catalysts represent a promising basis for further exploration for the selective oxidation of a range of feed stocks.

Acknowledgements The authors wish to acknowledge the financial support of and research discussion with Haldor Topsøe. We also thank Diamond Light Source (DLS) and electron Physical Science Imaging Centre (ePSIC) for access (Instrument E01 Session Number MG26190) and support that contributed to the results presented. XPS data collection was performed at the EPSRC National Facility for XPS ('HarwellXPS'), operated by Cardiff University and UCL, under Contract No. PR16195.

Compliance with Ethical Standards

Conflict of interest The authors declare no conflict of interests.

Open Access This article is licensed under a Creative Commons Attribution 4.0 International License, which permits use, sharing, adaptation, distribution and reproduction in any medium or format, as long as you give appropriate credit to the original author(s) and the source, provide a link to the Creative Commons licence, and indicate if changes were made. The images or other third party material in this article are included in the article's Creative Commons licence, unless indicated otherwise in a credit line to the material. If material is not included in the article's Creative Commons licence and your intended use is not permitted by statutory regulation or exceeds the permitted use, you will need to obtain permission directly from the copyright holder. To view a copy of this licence, visit <http://creativecommons.org/licenses/by/4.0/>.

References

- Hu B, Yuan Y, Xiao J, Guo C, Liu Q, Tan Z, Li Q (2008) Rational oxidation of cyclohexane to cyclohexanol, cyclohexanone and adipic acid with air over metalloporphyrin and cobalt salt. *J Porphyrins Phthalocyanines* 12:27–34
- Sun L, Liu J, Luo W, Yang Y, Wang F, Weerakkody C, Suib SL (2018) Preparation of amorphous copper - chromium oxides catalysts for selective oxidation of cyclohexane. *Mol Catal* 460:16–26
- Yu H, Peng F, Tan J, Hu X, Wang H, Yang J, Zheng W (2011) Selective Catalysis of the Aerobic Oxidation of Cyclohexane in the Liquid Phase by Carbon Nanotubes. *Angew Chem Int Ed* 50:3978–3982
- Wang T, She Y, Fu H, Li H (2016) Selective cyclohexane oxidation catalyzed by manganese porphyrins and co-catalysts. *Catal Today* 264:185–190
- Hermans I, Peeters J, Jacobs PA (2008) Origin of Byproducts during the Catalytic Autoxidation of Cyclohexane. *J Phys Chem A* 112:1747–1753
- Hermans I, Jacobs PA, Peeters J (2006) To the Core of Autocatalysis in Cyclohexane Autoxidation. *Chem–Eur J* 12:4229–4240
- Pires EL, Magalhães JC, Schuchardt U (2000) Effects of oxidant and solvent on the liquid-phase cyclohexane oxidation catalyzed by Ce-exchanged zeolite Y. *Appl Catal A* 203:231–237
- Ramanathan A, Hamdy MS, Parton R, Maschmeyer T, Jansen JC, Hanefeld U (2009) Co-TUD-1 catalysed aerobic oxidation of cyclohexane. *Appl Catal A* 355:78–82
- Jian J, Kuang D, Wang X, Zhou H, Gao H, Sun W, Yuan Z, Zeng J, You K, Luo H (2020) Highly dispersed Co/SBA-15 mesoporous materials as efficient and stable catalyst for partial

- oxidation of cyclohexane with molecular oxygen. *Mater Chem Phys* 246:122814
- Maksimchuk NV, Kovalenko KA, Fedin VP, Kholdeeva OA (2012) Cyclohexane selective oxidation over metal-organic frameworks of MIL-101 family: superior catalytic activity and selectivity. *Chem Commun* 48:6812–6814
 - Sun Z, Li G, Liu L, Liu H (2012) Au nanoparticles supported on Cr-based metal-organic framework as bimetallic catalyst for selective oxidation of cyclohexane to cyclohexanone and cyclohexanol. *Catal Commun* 27:200–205
 - Liu X, Conte M, Sankar M, He Q, Murphy DM, Morhan DJ, Jenkins RL, Knight D, Whiston K, Kiely CJ, Hutchings GJ (2015) Liquid phase oxidation of cyclohexane using bimetallic Au-Pd/MgO catalysts. *Appl Catal A* 504:373–380
 - Xu Y-J, Landon P, Enache D, Carley AF, Roberts MW, Hutchings GJ (2005) Selective conversion of cyclohexane to cyclohexanol and cyclohexanone using a gold catalyst under mild conditions. *Catal Lett* 101:175–179
 - Khare S, Shrivastava P (2016) Solvent-free oxidation of cyclohexane over covalently anchored transition-metal salicylaldehyde complexes to α -zirconium phosphate using tert-butylhydroperoxide. *J Mol Catal A: Chem* 411:279–289
 - Du Y, Xiong Y, Li J, Yang X (2009) Selective oxidation of cyclohexane with hydrogen peroxide in the presence of copper pyrophosphate. *J Mol Catal A: Chem* 298:12–16
 - Costa AA, Ghesti GF, de Macedo JL, Braga VS, Santos MM, Dias JA, Dias SCL (2008) Immobilization of Fe, Mn and Co tetraphenylporphyrin complexes in MCM-41 and their catalytic activity in cyclohexene oxidation reaction by hydrogen peroxide. *J Mol Catal A: Chem* 282:149–157
 - Scoville JR, Novicova IA (1996) Hydrogen peroxide disinfecting and sterilizing compositions. US5900256
 - Wegner P (2003) Hydrogen peroxide stabilizer and resulting product and applications. US20050065052A1
 - Crombie CM, Lewis RJ, Kovačič D, Morgan DJ, Davies TE, Edwards JK, Škjøth-Rasmussen MS, Hutchings GJ (2020) The Influence of Reaction Conditions on the Oxidation of Cyclohexane via the In-Situ Production of H₂O₂. *Catal Lett*. <https://doi.org/10.1007/s10562-020-03281-1>
 - Li G, Edwards J, Carley AF, Hutchings GJ (2007) Direct synthesis of hydrogen peroxide from H₂ and O₂ and in situ oxidation using zeolite-supported catalysts. *Catal Commun* 8:247–250
 - Sankar M, He Q, Morad MJ, Pritchard J, Freakley SJ, Edwards JK, Taylor SH, Morgan DJ, Carley AF, Knight DW, Kiely CJ, Hutchings GJ (2012) Synthesis of Stable Ligand-free Gold-Palladium Nanoparticles Using a Simple Excess Anion Method. *ACS Nano* 6:6600–6613
 - Santos A, Lewis RJ, Malta G, Howe AGR, Morgan DJ, Mapton E, Gaskin P, Hutchings GJ (2019) Direct synthesis of hydrogen peroxide over Au-Pd supported nanoparticles under ambient conditions. *Ind Eng Chem Res* 58:12623–12631
 - Edwards JK, Solsona BE, Landon P, Carley AF, Herzing A, Kiely CJ, Hutchings GJ (2005) Direct synthesis of hydrogen peroxide from H₂ and O₂ using TiO₂-supported Au-Pd catalysts. *J Catal* 236:69–79
 - Carabineiro SAC, Martins LMDRS, Avalos-Borja M, Buijnsters JG, Pombeiro AJL, Figueiredo JL (2013) Gold nanoparticles supported on carbon materials for cyclohexane oxidation with hydrogen peroxide. *Appl Catal A* 467:279–290
 - Edwards JK, Thomas A, Carley AF, Herzing AA, Kiely CJ, Hutchings GJ (2008) Au-Pd supported nanocrystals as catalysts for the direct synthesis of hydrogen peroxide from H₂ and O₂. *Green Chem* 10:388–394
 - Scoville JH (1976) Hartree-Slater subshell photoionization cross-sections at 1254 and 1487 eV. *J Electron Spectrosc Relat Phenom* 8:129–137
 - Liu Q, Bauer JC, Schaak RE, Lunsford JH (2008) Supported palladium nanoparticles: an efficient catalyst for the direct formation of H₂O₂ from H₂ and O₂. *Angew Chem Int Ed* 47(33):6221–6224
 - Arrigo R, Schuster ME, Abate S, Giorgianni G, Centi G, Perathoner S, Wrabetz S, Pfeifer V, Antonietti M, Schlögl R (2016) Pd Supported on Carbon Nitride Boosts the Direct Hydrogen Peroxide Synthesis. *ACS Catal* 6:6959–6966
 - Li J, Ishihara T, Yoshizawa K (2011) Theoretical Revisit of the Direct Synthesis of H₂O₂ on Pd and Au@Pd Surfaces: A Comprehensive Mechanistic Study. *J Phys Chem C* 115:25359–25367
 - Li J, Yoshizawa K (2015) Mechanistic aspects in the direct synthesis of hydrogen peroxide on PdAu catalyst from first principles. *Catal Today* 248:142–148
 - Landon P, Collier PJ, Carley AF, Chadwick D, Papworth AJ, Burrows A, Kiely CJ, Hutchings GJ (2003) Direct synthesis of hydrogen peroxide from H₂ and O₂ using Pd and Au catalysts. *Phys Chem Chem Phys* 5:1917–1923
 - Edwards JK, Solsona B, Ntainjua EN, Carley AF, Herzing AA, Kiely CJ, Hutchings GJ (2009) Switching off hydrogen peroxide hydrogenation in the direct synthesis process. *Science* 323:1037–1041
 - Lewis RJ, Hutchings GJ (2019) Recent Advances in the Direct Synthesis of H₂O₂. *ChemCatChem* 11:298–308
 - Cybula A, Priebe JB, Pohl M, Sobczak JW, Schneider M, Zielińska-Jurek A, Brückner A, Zaleska A (2014) The effect of calcination temperature on structure and photocatalytic properties of Au/Pd nanoparticles supported on TiO₂. *Appl Catal B*. <https://doi.org/10.1016/j.apcatb.2014.01.042>
 - Freakley SJ, He Q, Harrhy JH, Lu L, Crole DA, Morgan DJ, Ntainjua EN, Edwards JK, Carley AF, Borisevich AY, Kiely CJ, Hutchings GJ (2016) Palladium-tin catalysts for the direct synthesis of H₂O₂ with high selectivity. *Science* 351:965–968
 - Zhang J, Shao Q, Zhang Y, Bai S, Feng Y, Huang X (2018) Promoting the Direct H₂O₂ Generation Catalysis by Using Hollow Pd-Sn Intermetallic Nanoparticles. *Small* 14:1703990
 - Gu J, Wang S, He Z, Han Y, Zhang J (2016) Direct synthesis of hydrogen peroxide from hydrogen and oxygen over activated-carbon-supported Pd-Ag alloy catalysts. *Catal Sci Technol* 6:809–817
 - Wang S, Gao K, Li W, Zhang J (2017) Effect of Zn addition on the direct synthesis of hydrogen peroxide over supported palladium catalysts. *Appl Catal A* 531:89–95
 - Maity S, Eswaramoorthy M (2016) Ni-Pd bimetallic catalysts for the direct synthesis of H₂O₂ - unusual enhancement of Pd activity in the presence of Ni. *J Mater Chem A* 4:3233–3237
 - Crole DA, Underhill R, Edwards JK, Shaw G, Freakley SJ, Hutchings GJ, Lewis RJ (2020) The direct synthesis of hydrogen peroxide from H₂ and O₂ using Pd-Ni/TiO₂ catalysts. *Phil Trans R Soc* 378:20200062
 - Wang S, Lewis RJ, Doronkin DE, Morgan DJ, Grunwaldt J, Hutchings GJ, Behrens S (2020) The Direct Synthesis of Hydrogen Peroxide from H₂ and O₂ Using Pd-Ga and Pd-In Catalysts. *Catal Sci Technol*. <https://doi.org/10.1039/C9CY02210D>
 - Doronkin DE, Wang S, Sharapa DI, Deschner BJ, Sheppard TL, Zimina A, Studt F, Dittmeyer R, Behrens S, Grunwaldt J (2020) Dynamic structural changes of supported Pd, PdSn, and PdIn nanoparticles during continuous flow high pressure direct H₂O₂ synthesis. *Catal Sci Technol* 10:4726–4742
 - Ding D, Xu X, Tian P, Liu X, Xu J, Han Y (2018) Promotional effects of Sb on Pd-based catalysts for the direct synthesis of hydrogen peroxide at ambient pressure. *Chinese J Catal* 39:673–681
 - Tian P, Xu X, Ao C, Ding D, Li W, Si R, Tu W, Xu J, Han Y (2017) Direct and Selective Synthesis of Hydrogen Peroxide over Palladium-Tellurium Catalysts at Ambient Pressure. *ChemSuschem* 10:3342–3346

45. Costa RCC, Lelis MFF, Oliveira LCA, Fabris JD, Ardisson JD, Rios RRVA, Silva CN, Lago RM (2006) Novel active heterogeneous Fenton system based on $\text{Fe}_{3-x}\text{M}_x\text{O}_4$ (Fe Co, Mn, Ni): The role of M^{2+} species on the reactivity towards H_2O_2 reactions. *J Hazard Mater* 129:171–178
46. Liu Y, Yu Z, Hou Y, Peng Z, Wang L, Gong Z, Zhu J, Su D (2016) Highly efficient Pd-Fe/Ni foam as heterogeneous Fenton catalysts for the three-dimensional electrode system. *Catal Commun* 86:63–66
47. Gong X, Lewis RJ, Zhou S, Morgan DJ, Davies TE, Liu X, Kiely CJ, Zong B, Hutchings GJ (2020) Enhanced catalyst selectivity in the direct synthesis of H_2O_2 through Pt incorporation into TiO_2 supported AuPd catalysts. *Catal Sci Technol* 10:4635–4644
48. Ouyang L, Tian P, Da G, Xu X, Ao C, Chen T, Si R, Xu J, Han Y (2015) The origin of active sites for direct synthesis of H_2O_2 on Pd/ TiO_2 catalysts: Interfaces of Pd and PdO domains. *J Catal* 321:70–80
49. Meher S, Rana RK (2019) A rational design of a Pd-based catalyst with a metal–metal oxide interface influencing molecular oxygen in the aerobic oxidation of alcohols. *Green Chem* 21:2494–2503
50. Burch R, Ellis PR (2003) An investigation of alternative catalytic approaches for the direct synthesis of hydrogen peroxide from hydrogen and oxygen. *Appl Catal B* 42:203–211
51. Enache DI, Edwards JK, Landon P, Solsona-Espriu B, Carley AF, Herzing AA, Watanabe M, Kiely CJ, Knight DW, Hutchings GJ (2006) Solvent-free oxidation of primary alcohols to aldehydes using Au-Pd/ TiO_2 catalysts. *Science* 311:362–365
52. Kesavan L, Tiruvalam R, Rahim MHA, Saiman MI, Enache DI, Jenkins RL, Dimitratos N, Lopez-Sanchez JA, Taylor SH, Knight DW, Kiely CJ, Hutchings GJ (2011) Solvent-Free Oxidation of Primary Carbon-Hydrogen Bonds in Toluene Using Au-Pd Alloy Nanoparticles. *Science* 331:195–199
53. Ketchie WC, Murayama M, Davis RJ (2007) Selective oxidation of glycerol over carbon-supported AuPd catalysts. *J Catal* 250:264–273
54. Lewis RJ, Ueura K, Fukuta Y, Freakley SJ, Kang L, Wang R, He Q, Edwards JK, Yamamoto MDJ, Hutchings GJ (2019) The direct synthesis of H_2O_2 using TS-1 supported catalysts. *ChemCatChem* 11:1673–1680
55. Lewis RJ, Bara-Estaun A, Agarwal N, Freakley SJ, Morgan DJ, Hutchings GJ (2019) The Direct Synthesis of H_2O_2 and Selective Oxidation of Methane to Methanol Using HZSM-5 Supported AuPd Catalysts. *Catal Lett* 149:3066–3075
56. Pokutsa A, Kubaj Y, Zaborovskyi A, Maksym D, Paczesniak T, Mysliwiec B, Bidzinska E, Muzart J, Sobkowiak A (2017) V(IV)-catalyzed cyclohexane oxygenation promoted by oxalic acid: Mechanistic study. *Mol Catal* 434:194–205
57. Bellifa A, Lahcene D, Tchenar YN, Choukchou-Braham A, Bachir R, Bedrane S, Kappenstein C (2006) Preparation and characterization of 20wt.% V_2O_5 - TiO_2 catalyst oxidation of cyclohexane. *Appl Catal A* 305:1–6
58. Pillai UR, Sahle-Demessie E (2003) Vanadium phosphorus oxide as an efficient catalyst for hydrocarbon oxidations using hydrogen peroxide. *New J Chem* 27:525–528
59. Rezaei M, Najafi Chermahini A, Dabbagh HA (2017) Green and selective oxidation of cyclohexane over vanadium pyrophosphate supported on mesoporous KIT-6. *Chem Eng J* 314:515–525
60. Carvalho NMF, Horn A, Antunes OAC (2006) Cyclohexane oxidation catalyzed by mononuclear iron(III) complexes. *Appl Catal A* 305:140–145
61. Pal N, Pramanik M, Bhaumik A, Ali M (2014) Highly selective and direct oxidation of cyclohexane to cyclohexanone over vanadium exchanged NaY at room temperature under solvent-free conditions. *J Mol Catal A: Chem* 392:299–307
62. Makgwane PR, Ray SS (2014) Efficient room temperature oxidation of cyclohexane over highly active hetero-mixed $\text{WO}_3/\text{V}_2\text{O}_5$ oxide catalyst. *Catal Commun* 54:118–123
63. Martínez-Méndez S, Henríquez Y, Domínguez O, D’Ornelas L, Krentzien H (2006) Catalytic properties of silica supported titanium, vanadium and niobium oxide nanoparticles towards the oxidation of saturated and unsaturated hydrocarbons. *J Mol Catal A: Chem* 252:226–234
64. Fu X, Tang W, Ji L, Chen S (2012) $\text{V}_2\text{O}_5/\text{Al}_2\text{O}_3$ composite photocatalyst: Preparation, characterization, and the role of Al_2O_3 . *Chem Eng J* 180:170–177
65. Pillai UR, Sahle-Demessie E (2002) A highly efficient oxidation of cyclohexane over VPO catalysts using hydrogen peroxide. *Chem Commun* 18:2142–2143
66. Mahdavi V, Hasheminasab HR (2015) Liquid-phase efficient oxidation of cyclohexane over cobalt promoted VPO catalyst using tert-butylhydroperoxide. *J Taiwan Inst Chem Eng* 51:53–62
67. Liu Q, Gath KK, Bauer JC, Schaak RE, Lunsford JH (2009) The Active Phase in the Direct Synthesis of H_2O_2 from H_2 and O_2 over Pd/ SiO_2 Catalyst in a H_2SO_4 /Ethanol System. *Catal Lett* 132:342–348
68. Wang D, Kung HH, Barteau MA (2000) Identification of vanadium species involved in sequential redox operation of VPO catalysts. *Appl Catal A* 201:203–213
69. Biesinger MC, Lau LWM, Gerson AR, Smart RSC (2010) Resolving surface chemical states in XPS analysis of first row transition metals, oxides and hydroxides: Sc, Ti, V, Cu and Zn. *Appl Surf Sci* 257:887–898
70. Dissanayake DP, Lunsford JH (2002) Evidence for the Role of Colloidal Palladium in the Catalytic Formation of H_2O_2 from H_2 and O_2 . *J Catal* 206:173–176
71. Silva TFS, Leod TCOM, Martins LMDRS, Guedes da Silva MFC, Schiavon MA, Pombeiro AJL (2013) Pyrazole or tris(pyrazolyl) ethanol oxo-vanadium(IV) complexes as homogeneous or supported catalysts for oxidation of cyclohexane under mild conditions. *J Mol Catal A: Chem* 367:52–60

Publisher’s Note Springer Nature remains neutral with regard to jurisdictional claims in published maps and institutional affiliations.

Affiliations

Caitlin M. Crombie¹ · Richard J. Lewis¹ · Dávid Kovačič¹ · David J. Morgan^{1,2} · Thomas J. A. Slater³ · Thomas E. Davies¹ · Jennifer. K. Edwards¹ · Martin Skov Skjøth-Rasmussen⁴ · Graham J. Hutchings¹

✉ Graham J. Hutchings
Hutch@cardiff.ac.uk

¹ School of Chemistry, Cardiff University, Main Building,
Park Place, Cardiff CF10 3AT, UK

² HarwellXPS, Research Complex At Harwell (RCaH),
Didcot OX11 OFA, UK

³ Electron Physical Sciences Imaging Centre, Diamond Light
Source Ltd, Oxfordshire OX11 0DE, UK

⁴ Haldor Topsøe A/S, Haldor Topsøes Allé 1,
2800 Kongens Lyngby, Denmark